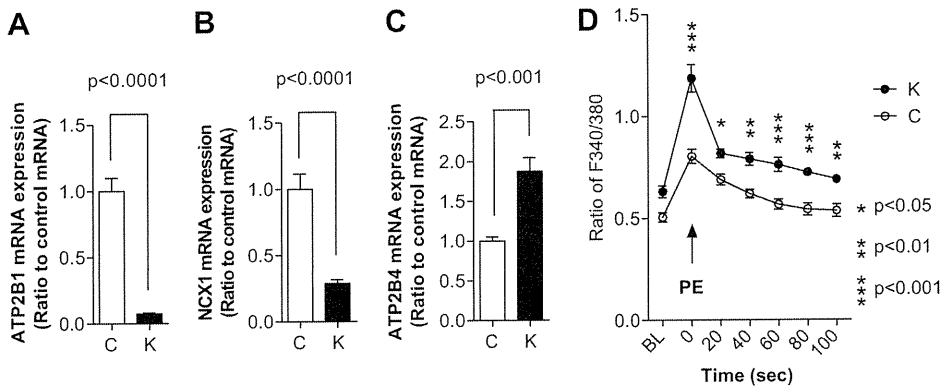

Figure 3. Altered gene expression and calcium transient in primary cultured vascular smooth muscle cells (VSMCs) of knockout (KO) mice. **A**, ATP2B1 mRNA expression in primary cultured VSMCs (n=8–10 for each genotype) quantified by quantitative RT-PCR (qRT-PCR) using exon 10 and 11 amplification. Data are presented as mean and SE ($P<0.0001$). **B**, NCX1 mRNA expression in primary cultured VSMCs (n=8–10 for each genotype) quantified by qRT-PCR. Data are presented as mean and SE ($P<0.0001$). **C**, ATP2B4 mRNA expression in primary cultured VSMCs (n=8–10 for each genotype) quantified by qRT-PCR. Data are presented as mean and SE ($P<0.0001$). **D**, Measurement of basal condition and phenylephrine-induced increase in intracellular calcium concentration of VSMCs were performed. Figure shows the time course of phenylephrine-stimulated change in intracellular calcium concentration in ATP2B1 KO VSMC and control VSMC mice (n=26–30 cells from 10 to 11 coverslips). ATP2B1 KO VSMC mice showed higher intracellular calcium concentration the entire time course before and after the phenylephrine stimulation. Data are displayed as ratio of F340/F380. Intracellular calcium concentration values over the entire cell were averaged to obtain the changes in the whole-cell calcium concentration. Data are presented as mean and SE (BL indicates baseline condition; PE, phenylephrine; K, ATP2B1 KO VSMC; C, control VSMC; $*P<0.05$, $**P<0.01$, $***P<0.001$).

showed an elevation in blood pressure associated with a rise in intracellular calcium and a decrease in NCX1 mRNA expression. Moreover, the vascular contractile response was increased in KO mice. These results suggest that ATP2B1 has important roles in calcium handling and contraction in VSMCs.

Important Relationship Between ATP2B1 and Other Calcium-Related Genes

NCX1, a calcium pump similar to ATP2B1, is known to play an important role in hypertension through its effect on VSMCs.[19,20] Interestingly, a recent report revealed that calcium clearance proteins, such as plasma membrane Ca^{2+}-ATPase (PMCA), sarcoplasmic reticulum Ca^{2+} ATPase, and NCX1, showed coordinated expression.[21] Furthermore, PMCA and NCX1 showed similar changes in expression in human arterial myocytes.[22] These recent findings suggest that ATP2B1 and NCX1 have a strong relationship and are modulated by the same system. Moreover, NCX1 and PMCA showed colocalization in the basolateral membrane of mouse distal convoluted cells in several studies.[23,24] Furthermore, several proteins associate with NCX1 and PMCA with an alteration in their activity.[25] On the contrary, ATP2B4 was upregulated in KO VSMCs. This upregulation of ATP2B4 seems to compensate for the decrease in expression of ATP2B1. These findings suggest that decreased expression of ATP2B1 and NCX1 is one of the possible mechanisms of increase in intracellular calcium concentration.

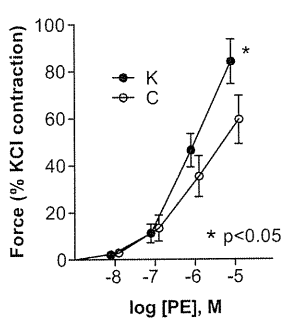

Figure 4. Phenylephrine-induced vasoconstriction of femoral artery rings. Isolated femoral artery rings obtained from knockout (KO) mice and control mice were stimulated with the α1-adrenoceptor agonist phenylephrine. Data are presented as mean and SE of 9 to 10 independent experiments. Force is expressed as the percentage of maximal contraction obtained by potassium-enriched solution.

Possibility of Alteration in Intracellular Calcium Homeostasis

In a recent study, a novel PMCA1 selective inhibitor, caloxin1b3, raised cytosolic calcium concentration in endothelial cells.[26] This finding supports the results that KO of ATP2B1 in VSMCs causes significant alterations in calcium-related gene expression and in intracellular calcium concentration. In the present study, KO VSMCs showed higher intracellular calcium concentration compared with the control, and a higher response was observed in response to the stimulation of phenylephrine compared with that of control VSMCs. Because increased intracellular calcium concentration may lead to blood pressure elevation via vasoconstriction,[27] the increased calcium concentrations seen in ATP2B1 KO VSMCs may be one of the possible mechanisms of high blood pressure seen in AP2B1 KO mice.

Increased Vasoconstriction Is One of the Possible Mechanisms for Blood Pressure Elevation

In the present study, we confirmed an increased contractile response to phenylephrine in femoral artery rings of KO

mice. Because phenylephrine activates inositol 1,4,5-triphosphate-induced intracellular calcium release and also stimulates voltage-independent calcium-permeable channels,[28] the alteration in contractile response may be attributed to alteration in intracellular calcium homeostasis. As shown in the present study, increased intracellular calcium concentration would augment the contractile capacity, which might increase the blood pressure in ATP2B1 KO mice. These findings strongly support the hypothesis that ATP2B1 gene is associated with blood pressure control in vivo.

Conclusion

We revealed that ATP2B1 KO in VSMCs increases the blood pressure in vivo study. Lack of ATP2B1 in VSMCs also increased intracellular calcium concentration and augmented the vascular contractility in ex vivo study. Our results clearly demonstrated that ATP2B1 gene expression in VSMCs is important in blood pressure regulation. Because the ATP2B1 gene has been reported to be a hypertension-susceptible gene by our systemic multiple candidate gene analyses, the present data suggest not only the importance of the ATP2B1 gene as a hypertension-related gene but also the value of the systemic multiple candidate gene approach and genome-wide association study in finding disease-related genes.

Perspectives

We made mice with conditional KO of ATP2B1 in VSMCs. However, the role of ATP2B1 in cells other than VSMCs in blood pressure control is not known. Thus, we need to further investigate the role of the ATP2B1 gene using other types of Cre mice and should make new organ-specific KO mice to analyze the role of the ATP2B1 gene in other conditions.

Sources of Funding

This work was supported by grants for scientific research (KAKENHI and Priority Areas "Medical Genome Science [Millennium Genome Project]" and "Applied Genomics") from the Ministry of Education, Culture, Sports, Science, and Technology, Japan; a grant for a Science and Technology Incubation Program in Advanced Regions, Japan Science and Technology Agency; a grant for scientific research from Yokohama City University; and a research grant from Olympus Corporation.

Disclosures

N.H., Y.T., K.K., Y.K., H.U., T.M., and S.U. have been named as the inventors on a patent application by Ehime University, Shiga University of Medical Science, and Yokohama City University in work related to this study.

References

1. Lifton RP. Molecular genetics of human blood pressure variation. *Science*. 1996;272:676–680.
2. Kohara K, Tabara Y, Nakura J, Imai Y, Ohkubo T, Hata A, Soma M, Nakayama T, Umemura S, Hirawa N, Ueshima H, Kita Y, Ogihara T, Katsuya T, Takahashi N, Tokunaga K, Miki T. Identification of hypertension-susceptibility genes and pathways by a systemic multiple candidate gene approach: the Millennium Genome Project for Hypertension. *Hypertens Res*. 2008;31:203–212.
3. Levy D, Ehret GB, Rice K, Verwoert GC, Launer LJ, Dehghan A, Glazer NL, Morrison AC, Johnson AD, Aspelund T, Aulchenko Y, Lumley T, Kottgen A, Vasan RS, Rivadeneira F, Eiriksdottir G, Guo X, Arking DE, Mitchell GF, Mattace-Raso FU, Smith AV, Taylor K, Scharpf RB, Hwang SJ, Sijbrands EJ, Bis J, Harris TB, Ganesh SK, O'Donnell CJ, Hofman A, Rotter JI, Coresh J, Benjamin EJ, Uitterlinden AG, Heiss G, Fox CS, Witteman JC, Boerwinkle E, Wang TJ, Gudnason V, Larson MG, Chakravarti A, Psaty BM, van Duijn CM. Genome-wide association study of blood pressure and hypertension. *Nat Genet*. 2009;41:677–687.
4. Cho YS, Go MJ, Kim YJ, Heo JY, Oh JH, Ban HJ, Yoon D, Lee MH, Kim DJ, Park M, Cha SH, Kim JW, Han BG, Min H, Ahn Y, Park MS, Han HR, Jang HY, Cho EY, Lee JE, Cho NH, Shin C, Park T, Park JW, Lee JK, Cardon L, Clarke G, McCarthy MI, Lee JY, Oh B, Kim HL. A large-scale genome-wide association study of Asian populations uncovers genetic factors influencing eight quantitative traits. *Nat Genet*. 2009;41:527–534.
5. Hong KW, Go MJ, Jin HS, Lim JE, Lee JY, Han BG, Hwang SY, Lee SH, Park HK, Cho YS, Oh B. Genetic variations in ATP2B1, CSK, ARSG and CSMD1 loci are related to blood pressure and/or hypertension in two Korean cohorts. *J Hum Hypertens*. 2010;24:367–372.
6. Hong KW, Jin HS, Lim JE, Kim S, Go MJ, Oh B. Recapitulation of two genomewide association studies on blood pressure and essential hypertension in the Korean population. *J Hum Genet*. 2010;55:336–341.
7. Takeuchi F, Isono M, Katsuya T, Yamamoto K, Yokota M, Sugiyama T, Nabika T, Fujioka A, Ohnaka K, Asano H, Yamori Y, Yamaguchi S, Kobayashi S, Takayanagi R, Ogihara T, Kato N. Blood pressure and hypertension are associated with 7 loci in the Japanese population. *Circulation*. 2010;121:2302–2309.
8. Okunade GW, Miller ML, Pyne GJ, Sutliff RL, O'Connor KT, Neumann JC, Andringa A, Miller DA, Prasad V, Doetschman T, Paul RJ, Shull GE. Targeted ablation of plasma membrane Ca^{2+}-ATPase (PMCA) 1 and 4 indicates a major housekeeping function for PMCA1 and a critical role in hyperactivated sperm motility and male fertility for PMCA4. *J Biol Chem*. 2004;279:33742–33750.
9. Liu L, Ishida Y, Okunade G, Shull GE, Paul RJ. Role of plasma membrane Ca^{2+}-ATPase in contraction-relaxation processes of the bladder: evidence from pmca gene-ablated mice. *Am J Physiol Cell Physiol*. 2006;290:C1239–1247.
10. Tabara Y, Kohara K, Kita Y, Hirawa N, Katsuya T, Ohkubo T, Hiura Y, Tajima A, Morisaki T, Miyata T, Nakayama T, Takashima N, Nakura J, Kawamoto R, Takahashi N, Hata A, Soma M, Imai Y, Kokubo Y, Okamura T, Tomoike H, Iwai N, Ogihara T, Inoue I, Tokunaga K, Johnson T, Caulfield M, Umemura S, Ueshima H, Miki T. Common variants in the ATP2B1 gene are associated with susceptibility to hypertension: the Japanese Millennium Genome Project. *Hypertension*. 2010;56:973–980.
11. Tsurumi Y, Tamura K, Tanaka Y, Koide Y, Sakai M, Yabana M, Noda Y, Hashimoto T, Kihara M, Hirawa N, Toya Y, Kiuchi Y, Iwai M, Horiuchi M, Umemura S. Interacting molecule of AT1 receptor, ATRAP, is colocalized with AT1 receptor in the mouse renal tubules. *Kidney Int*. 2006;69:488–494.
12. Sakai M, Tamura K, Tsurumi Y, Tanaka Y, Koide Y, Matsuda M, Ishigami T, Yabana M, Tokita Y, Hiroi Y, Komuro I, Umemura S. Expression of MAK-V/Hunk in renal distal tubules and its possible involvement in proliferative suppression. *Am J Physiol Renal Physiol*. 2007;292:F1526–F1536.
13. Mills PA, Huetteman DA, Brockway BP, Zwiers LM, Gelsema AJ, Schwartz RS, Kramer K. A new method for measurement of blood pressure, heart rate, and activity in the mouse by radiotelemetry. *J Appl Physiol*. 2000;88:1537–1544.
14. Kobayashi M, Inoue K, Warabi E, Minami T, Kodama T. A simple method of isolating mouse aortic endothelial cells. *J Atheroscler Thromb*. 2005;12:138–142.
15. Zimmerman MC, Sharma RV, Davisson RL. Superoxide mediates angiotensin II-induced influx of extracellular calcium in neural cells. *Hypertension*. 2005;45:717–723.
16. Akaike T, Jin MH, Yokoyama U, Izumi-Nakaseko H, Jiao Q, Iwasaki S, Iwamoto M, Nishimaki S, Sato M, Yokota S, Kamiya Y, Adachi-Akahane S, Ishikawa Y, Minamisawa S. T-type Ca^{2+} channels promote oxygenation-induced closure of the rat ductus arteriosus not only by vasoconstriction but also by neointima formation. *J Biol Chem*. 2009;284:24025–24034.
17. Carafoli E. The Ca^{2+} pump of the plasma membrane. *J Biol Chem*. 1992;267:2115–2118.
18. Pande J, Szewczyk MM, Kuszczak I, Grover S, Escher E, Grover AK. Functional effects of Caloxin 1c2, a novel engineered selective inhibitor of plasma membrane Ca^{2+}-pump isoform 4, on coronary artery. *J Cell Mol Med*. 2008;12:1049–1060.

19. Iwamoto T, Kita S, Zhang J, Blaustein MP, Arai Y, Yoshida S, Wakimoto K, Komuro I, Katsuragi T. Salt-sensitive hypertension is triggered by Ca^{2+} entry via Na^{+}/Ca^{2+} exchanger type-1 in vascular smooth muscle. *Nat Med.* 2004;10:1193–1199.
20. Blaustein MP. Sodium ions, calcium ions, blood pressure regulation, and hypertension: a reassessment and a hypothesis. *Am J Physiol.* 1977;232: C165–C173.
21. Pritchard TJ, Bowman PS, Jefferson A, Tosun M, Lynch RM, Paul RJ. Na^{+}-K^{+}-atpase and Ca^{2+} clearance proteins in smooth muscle: a functional unit. *Am J Physiol Heart Circ Physiol.* 2010;299:H548–H556.
22. Baryshnikov SG, Pulina MV, Zulian A, Linde CI, Golovina VA. Orai1, a critical component of store-operated Ca^{2+} entry, is functionally associated with $Na^{-}/Ca2^{+}$ exchanger and plasma membrane Ca^{2+} pump in proliferating human arterial myocytes. *Am J Physiol Cell Physiol.* 2009; 297:C1103–C1112.
23. Magyar CE, White KE, Rojas R, Apodaca G, Friedman PA. Plasma membrane Ca^{2+}-ATPase and NCX1 Na^{-}/Ca^{2+} exchanger expression in distal convoluted tubule cells. *Am J Physiol Renal Physiol.* 2002;283: F29–F40.
24. Loffing J, Loffing-Cueni D, Valderrabano V, Klausli L, Hebert SC, Rossier BC, Hoenderop JG, Bindels RJ, Kaissling B. Distribution of transcellular calcium and sodium transport pathways along mouse distal nephron. *Am J Physiol Renal Physiol.* 2001;281:F1021–F1027.
25. Ruknudin AM, Lakatta EG. The regulation of the Na^{+}/Ca^{2+} exchanger and plasmalemmal Ca^{2+} ATPase by other proteins. *Ann NY Acad Sci.* 2007;1099:86–102.
26. Szewczyk MM, Pande J, Akolkar G, Grover AK. Caloxin 1b3: a novel plasma membrane Ca^{2+}-pump isoform 1 selective inhibitor that increases cytosolic Ca^{2+} in endothelial cells. *Cell Calcium.* 2010;48: 352–357.
27. Brenner R, Perez GJ, Bonev AD, Eckman DM, Kosek JC, Wiler SW, Patterson AJ, Nelson MT, Aldrich RW. Vasoregulation by the $\beta 1$ subunit of the calcium-activated potassium channel. *Nature.* 2000; 407:870–876.
28. McDaniel SS, Platoshyn O, Wang J, Yu Y, Sweeney M, Krick S, Rubin LJ, Yuan JX. Capacitative Ca^{2+} entry in agonist-induced pulmonary vasoconstriction. *Am J Physiol Lung Cell Mol Physiol.* 2001;280: L870–L880.

Online Supplement

Title

Mice lacking hypertension candidate gene ATP2B1 in vascular smooth muscle cells show significant blood pressure elevation

Authors

Yusuke Kobayashi[1)], Nobuhito Hirawa[2)], Yasuharu Tabara[3)], Hidenori Muraoka[4)], Megumi Fujita[1)], Nobuko Miyazaki[1)], Akira Fujiwara[1)], Yasuhiro Ichikawa[5)], Yuichiro Yamamoto[2)], Naoaki Ichihara[1)], Sanae Saka[1)], Hiromichi Wakui[1)], Shin-ichiro Yoshida[1)], Keisuke Yatsu[2)], Yoshiyuki Toya[1)], Gen Yasuda[2)], Katsuhiko Kohara[3)], Yoshikuni Kita[6)], Kohtaro Takei[4)], Yoshio Goshima[4)], Yoshihiro Ishikawa[5)], Hirotsugu Ueshima[6)], Tetsuro Miki[3)], Satoshi Umemura[1)]

Affiliations

1. Department of Medical Science and Cardiorenal Medicine, Yokohama City University Graduate School of Medicine, Yokohama, Japan
2. Division of Nephrology and Hypertension, Yokohama City University Medical Center, Yokohama, Japan
3. Department of Geriatric Medicine, Ehime University Graduate School of Medicine, Toon, Japan
4. Department of Molecular Pharmacology and Neurobiology, Yokohama City University Graduate School of Medicine, Yokohama, Japan
5. Cardiovascular Research Institute, Yokohama City University Graduate School of Medicine, Yokohama, Japan
6. Department of Health Science, Shiga University of Medical Science, Otsu, Japan

METHODS

Animal Care

Animals were housed under a 12-hour day/night cycle at a temperature of 25°C. Tap water was provided *ad libitum*. Experiments were conducted under the guidelines for animal experiments set by the Animal Experiment Committee of Yokohama City University School of Medicine. In order to clarify the importance of the ATP2B1 gene in blood pressure regulation, we attempt to knock out the function of the ATP2B1 gene

of vascular smooth muscle cells. To generate conditional ATP2B1 KO mice, we utilized the Cre-loxP and FLP-FRT recombination system.

Cre-Mice

SM22-Cre mice [Tg(Tagln-cre)1Her/J, stock #004746] were obtained from The Jackson Laboratory (Bar Harbor, ME, USA). The SM22-Cre transgenic mice express Cre recombinase under control of the mouse transgelin (smooth muscle protein 22-alpha) promoter. Thus SM22-Cre mice knockout the gene that is sandwiched with loxP sites in vascular smooth muscle cell (VSMC) specifically. Mice engineered in this study were backcrossed onto the (C57BL/6J) genetic background for at least six generations.

ATP2B1 conditional knockout (KO) mouse

Conditional ATP2B1 KO mouse was generated by Cre/loxP and FLP-FRT recombination system. ATP2B1 is encoded by 21 exons on chromosome 10, and mice lacking exon 10 was reported to be an embryonic lethal. We therefore designed a new vector to knockout the exon 10 of ATP2B1 gene (Figure S1). This targeting vector contains a loxP-FRT-PGK-neo-FRT cassette with 5,572 bp of ATP2B1 homologous regions upstream of exon 10, and loxP site with 3,891 bp homologous regions downstream of exon 10. After linearization and electroporation into the C57BL/6 (RENKA) ES cell lines (Transgenic Inc., Kumamoto, Japan), 431 neo-resistant ES cell clones were obtained. Among the randomly selected 143 ES clones, homologous recombination was confirmed in six clones (#73583, #73584, #73588, #73612, #73693, #73697) by KpnI or PvuII digested Southern blot analysis using 5' probe, 3' probe or neo probe (Figure S2, S3, S4). To verify the recombination of loxP site downstream exon 10, PCR-amplified fragment length (using primer A and primer B) was analyzed by agarose-gel electrophoresis (Figure S5). Both wild-type allele (460 bp) and mutant allele (519 bp) was ascertained in all six clones. We next eliminated the PGK-neo region by transfection of Flp recombinase vector in to the #73588 clone (Figure S6). Flp/FRT recombination was verified by analyzing the length of PCR product amplified with primer C and primer D (Figure S7). Among 104 transfected clones, recombination was ascertained in the seven clones (#77743, #77775, #77936, #77937, #77956, #77961, #77964). KpnI or EcoRI digested Southern blot analysis using 5' probe, 3' probe, or DR probe further confirmed the Flp/FRT recombination in all seven clones (Figure S8). Three ATP2B1floxed ES cell clones (#77743, #77775, #77936) were aggregated with 8-cell stage embryos (ICR strain). The embryo was transferred into uterus of recipient females, and chimeras were delivered by Caesarean section at embryonic 17 day. The

chimeras were mated with wild-type mouse, and germline transmission was ascertained in 14 (9 male, and 5 female) of 31 F1 mouse.

Creation of the Vascular Smooth Muscle Cell-targeted ATP2B1 KO Mice

$ATP2B1^{loxP/loxP}$ mice were generated by the Cre-loxP and FLP-FRT recombination system. ATP2B1 is encoded by 21 exons on chromosome 10, and mice lacking exon 10 are reported to be embryo-lethal. We therefore designed a vector to knockout exon 10 of the ATP2B1 gene. To target inactivation of the ATP2B1 gene to VSMC, $ATP2B1^{loxP/loxP}$ mice were intercrossed with SM22-Cre transgenic mice expressing Cre recombinase under control of the mouse transgelin (smooth muscle protein 22-alpha) promoter. The resulting $ATP2B1^{loxP/-}$/SM22-Cre animals were further mated with $ATP2B1^{loxP/loxP}$ mice to generate $ATP2B1^{loxP/loxP}$/SM22-Cre (VSMC ATP2B1 KO) mice and $ATP2B1^{loxP/loxP}$ mice without SM22-Cre (control mice). Animals used for experiments were backcrossed at least 6 times.

Blood Pressure Measured by Radiotelemetric Method

Direct blood pressure measurement was performed by a radiotelemetric method in which a blood pressure transducer (PA-C10, Data Sciences International, USA) was inserted into the left carotid artery. Ten days after transplantation, each mouse was housed individually in a standard cage on a receiver under a 12-hour light-dark cycle. Direct blood pressure was recorded every minute by radiotelemetry, as described previously [1].

Cell Culture of Mouse VSMC

The VSMC were aseptically isolated from thoracic aortic explants of an 8-week-old ATP2B1 KO mouse and its wild-type littermate as described previously [2]. VSMC were prepared by the explant method and cultured in Dulbecco's modified Eagle's Medium as described previously [3, 4]. VSMC multiplying in a medium containing FBS rapidly lose their contractile features and become "synthetic" cells [3]. Thus, the early passage cells (third to sixth passage) were used in the present study. Subconfluent VSMC were used in the following experiments. The serum of these cells were deprived for 24 hours and then stimulated as indicated. After the desired incubation period, cells were rinsed with ice-cold phosphate-buffered saline and then lysed and sonicated.

Western Blot Analysis of ATP2B1

Western blot analysis was performed as described previously [5, 6]. Briefly, tissue extracts

were used for electrophoresis, and membranes (Millipore, USA) were incubated with rabbit polyclonal anti-ATP2B1 antibody (MBL, Japan) and subjected to enhanced chemiluminescence (GE Healthcare, US). The images were analyzed quantitatively using a FUJI LAS3000 Image Analyzer (FUJI Film, Japan) for determination of the ATP2B1 protein level. To measure the aortic expression ratio of ATP2B1/β-actin, each ATP2B1 protein level was divided by the corresponding β-actin protein level obtained by re-probing, and thus derived from the same extract.

Isometric Tension of the Femoral Artery Vascular Rings

After the mice were anesthetized with pentobarbital, the femoral artery ring was isolated and placed in a tissue bath and kept at 37° C. Two tungsten wires (40 μm in diameter) were threaded into the lumen, and the preparation was mounted in a two-channel myograph (Dual Wire myograph system 410A; Danish Myo Technology, Aarhus, Denmark). One tungsten wire was connected to a micro-manipulator, and the other was connected to a force transducer. All of the vascular rings were initially stabilized for at least 60 min with a modified Krebs-Henseleit solution (Sigma-Aldrich) whose temperature was maintained at 37 °C by a heated water jacket. Isometric tension was continuously monitored using a PowerLab/8 SP system (ADInstruments, Inc., Colorado Springs, CO). After the vascular ring was relaxed, the resting tension was adjusted to 5 mN. After normalization, phenylephrine (Sigma-Aldrich) was added to stimulate vasoconstriction. The concentration of phenylephrine was increased from 10^{-8} M to 10^{-5} M. After a plateau vasoconstriction had been attained, phenylephrine was washed out. At the end of all experiments, vasoconstriction of the femoral artery ring was induced by potassium-enriched solutions containing (in mM): KCl 120, $CaCl_2$ 2.5, $MgSO_4$ 1.17, $NaHCO_3$ 25, KH_2PO_4 1.18, EDTA 0.027, Glucose 5.5.

RESULTS

VSMC ATP2B1 KO Mice showed Higher Blood Pressure Assessed by 24-hour Radiotelemetric System than Control Mice

To confirm the effects of deletion of vascular smooth muscle cell ATP2B1 on blood pressure and to analyze the circadian pattern of blood pressure, conscious VSMC ATP2B1 KO mice and control mice were subjected to blood pressure measurements by radiotelemetry. KO mice showed higher blood pressure than control mice at 14 weeks of age throughout the day (diastolic blood pressure; Figure S9A, mean blood pressure;

Figure S9B).

REFERENCES

1. Mills PA, Huetteman DA, Brockway BP, Zwiers LM, Gelsema AJ, Schwartz RS, Kramer K: A new method for measurement of blood pressure, heart rate, and activity in the mouse by radiotelemetry. *J Appl Physiol.* 2000;88:1537-1544.
2. Kobayashi M, Inoue K, Warabi E, Minami T, Kodama T: A simple method of isolating mouse aortic endothelial cells. *J Atheroscler Thromb.* 2005;12:138-142.
3. Hashimoto T, Kihara M, Sato K, Imai N, Tanaka Y, Sakai M, Tamura K, Hirawa N, Toya Y, Kitamura H, Umemura S: Heparin recovers AT1 receptor and its intracellular signal transduction in cultured vascular smooth muscle cells. *FEBS Lett.* 2005;579:281-284.
4. Hashimoto T, Kihara M, Yokoyama K, Fujita T, Kobayashi S, Matsushita K, Tamura K, Hirawa N, Toya Y, Umemura S: Lipoxygenase products regulate nitric oxide and inducible nitric oxide synthase production in interleukin-1beta stimulated vascular smooth muscle cells. *Hypertens Res.* 2003;26:177-184.
5. Tsurumi Y, Tamura K, Tanaka Y, Koide Y, Sakai M, Yabana M, Noda Y, Hashimoto T, Kihara M, Hirawa N, Toya Y, Kiuchi Y, Iwai M, Horiuchi M, Umemura S: Interacting molecule of AT1 receptor, atrap, is colocalized with AT1 receptor in the mouse renal tubules. *Kidney Int.* 2006;69:488-494.
6. Tanaka Y, Tamura K, Koide Y, Sakai M, Tsurumi Y, Noda Y, Umemura M, Ishigami T, Uchino K, Kimura K, Horiuchi M, Umemura S: The novel angiotensin II type 1 receptor (at1r)-associated protein atrap downregulates at1r and ameliorates cardiomyocyte hypertrophy. *FEBS Lett.* 2005;579:1579-1586.

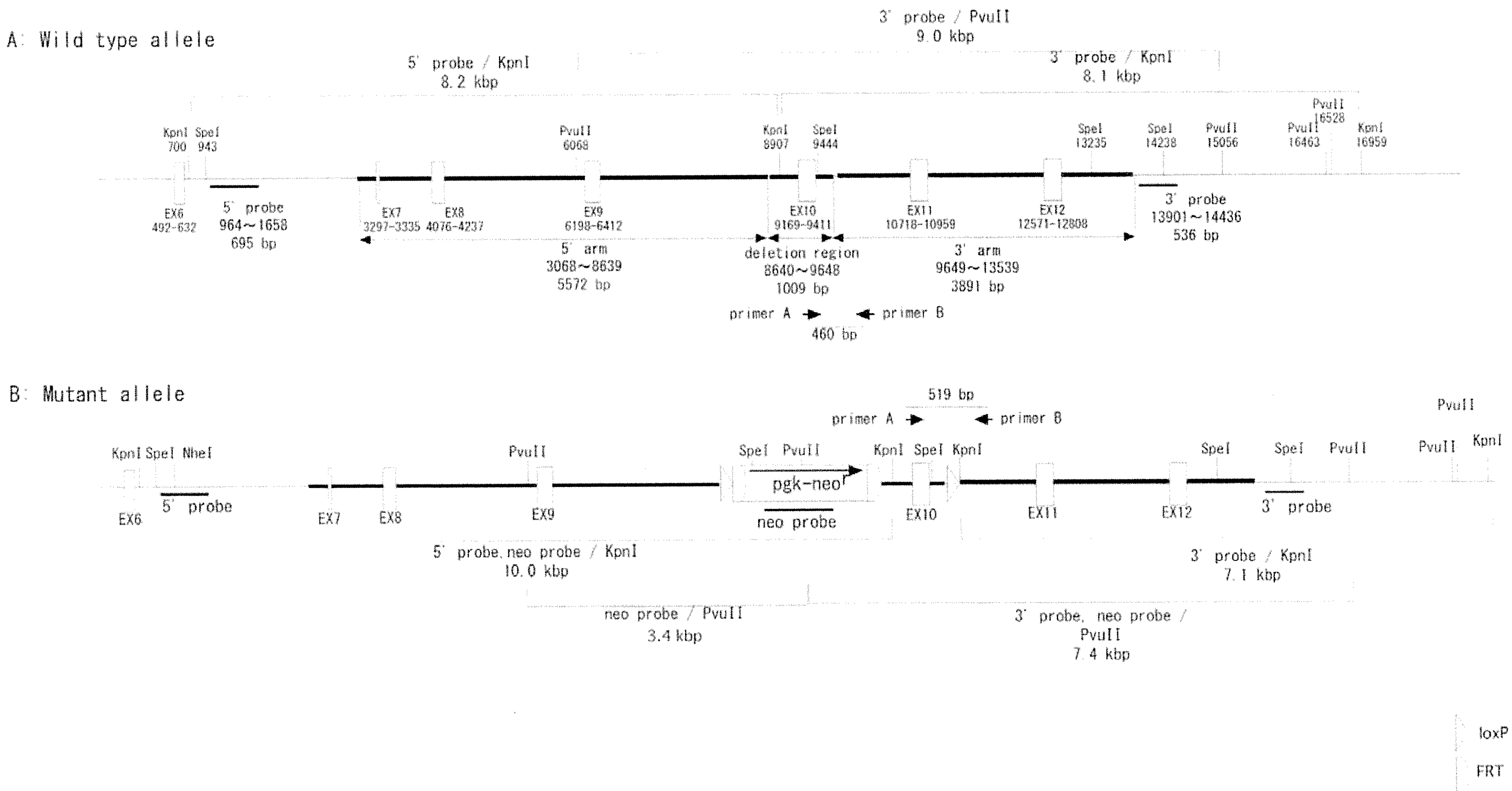
A: Wild type allele
3' probe / PvuII
9.0 kbp
5' probe / KpnI
8.2 kbp
3' probe / KpnI
8.1 kbp
KpnI 700
SpeI 943
PvuII 6068
KpnI 8907
SpeI 9444
SpeI 13235
SpeI 14238
PvuII 15056
PvuII 16463
PvuII 16528
KpnI 16959
EX6 492-632
5' probe 964~1658 695 bp
EX7 3297-3335
EX8 4076-4237
EX9 6198-6412
EX10 9169-9411
EX11 10718-10959
EX12 12571-12808
3' probe 13901~14436 536 bp
5' arm 3068~8639 5572 bp
deletion region 8640~9648 1009 bp
3' arm 9649~13539 3891 bp
primer A
primer B
460 bp
B: Mutant allele
519 bp
primer A
primer B
KpnI SpeI NheI
PvuII
SpeI PvuII
pgk-neo^r
KpnI SpeI KpnI
SpeI
SpeI PvuII
PvuII KpnI
PvuII
EX6
5' probe
EX7
EX8
EX9
neo probe
EX10
EX11
EX12
3' probe
5' probe, neo probe / KpnI
10.0 kbp
3' probe / KpnI
7.1 kbp
neo probe / PvuII
3.4 kbp
3' probe, neo probe / PvuII
7.4 kbp
loxP
FRT

Figure S1 Vector design of ATP2B1 exon 10 conditional KO mouse

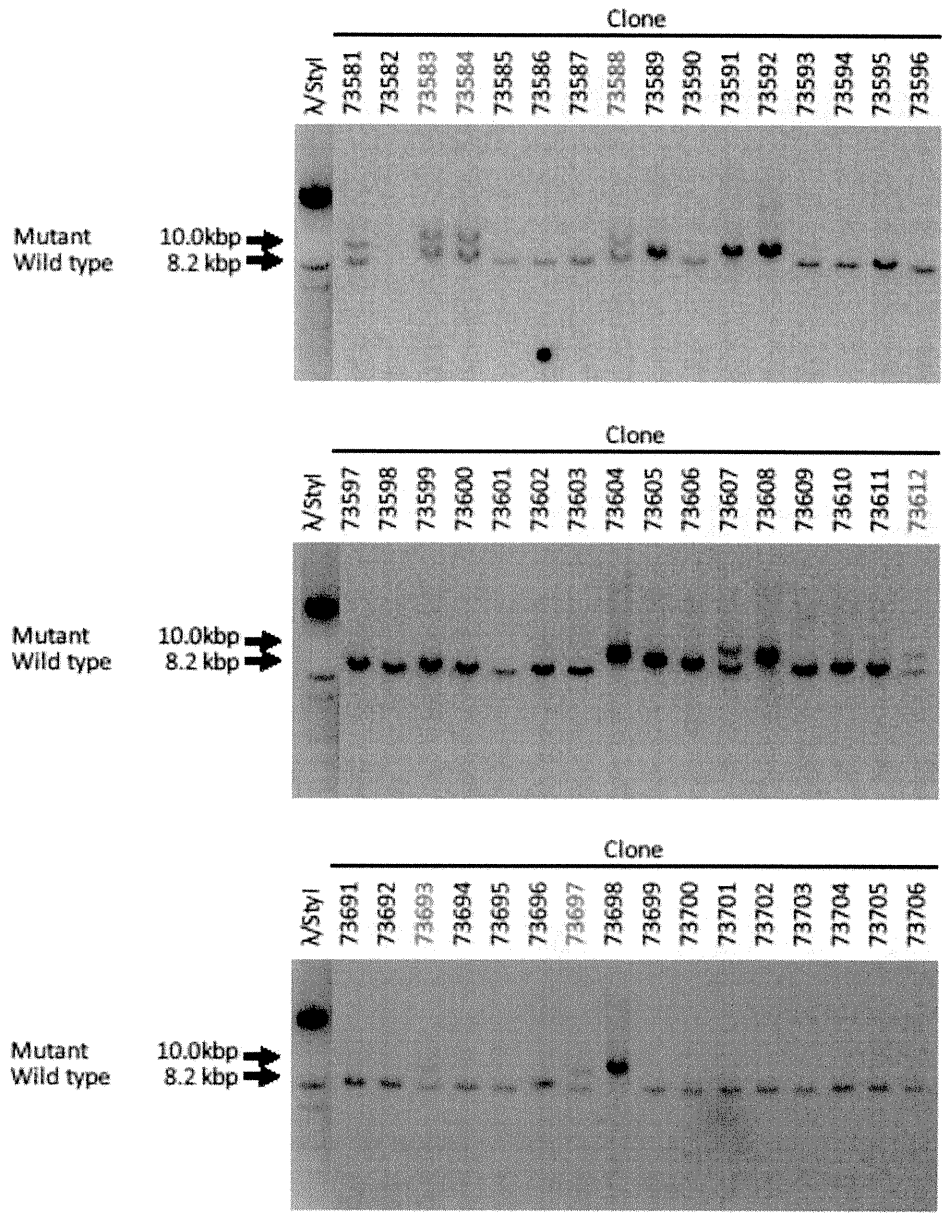

Figure S2 Kpn I-digested Southern blot analysis using 5' probe

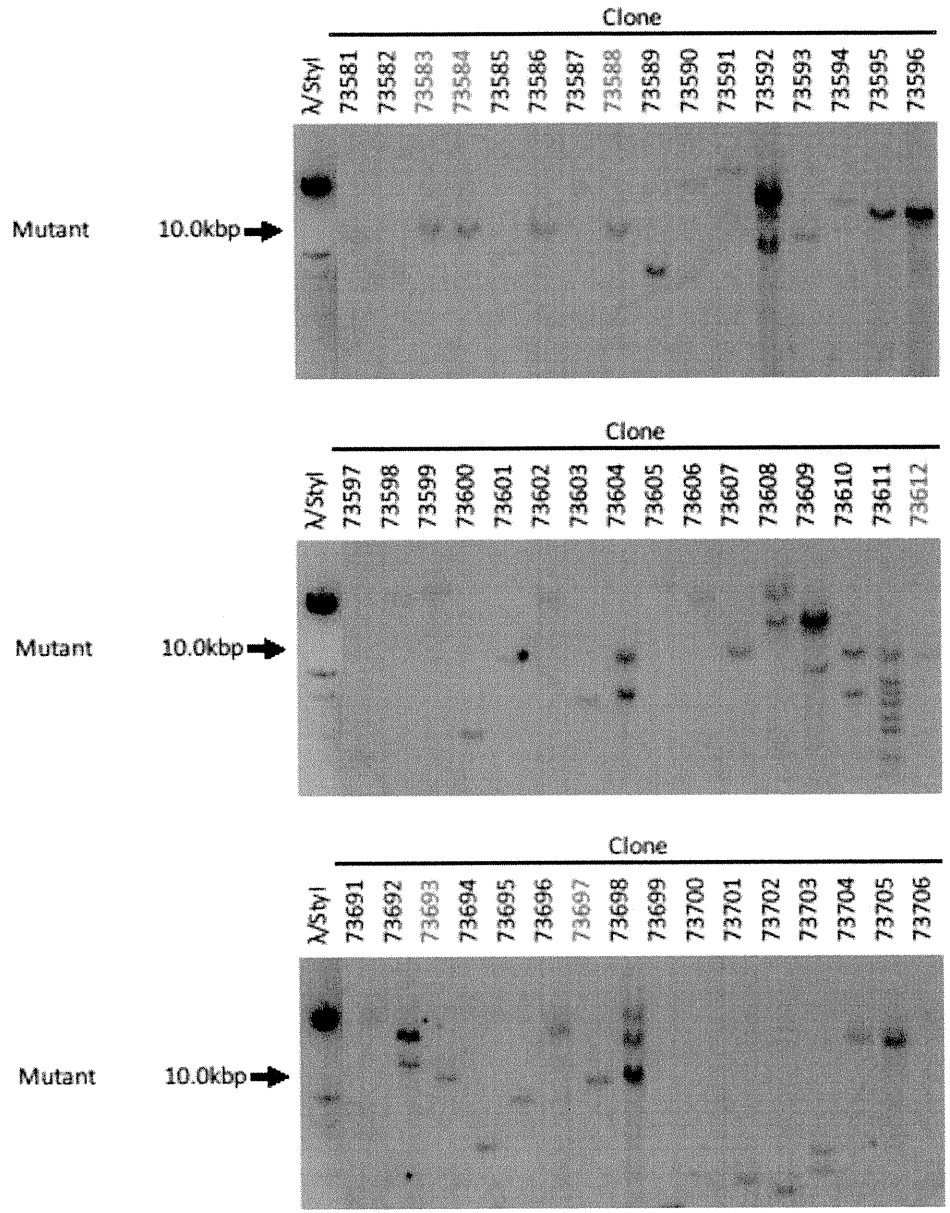

Figure S3 Kpn I-digested Southern blot analysis using neo probe

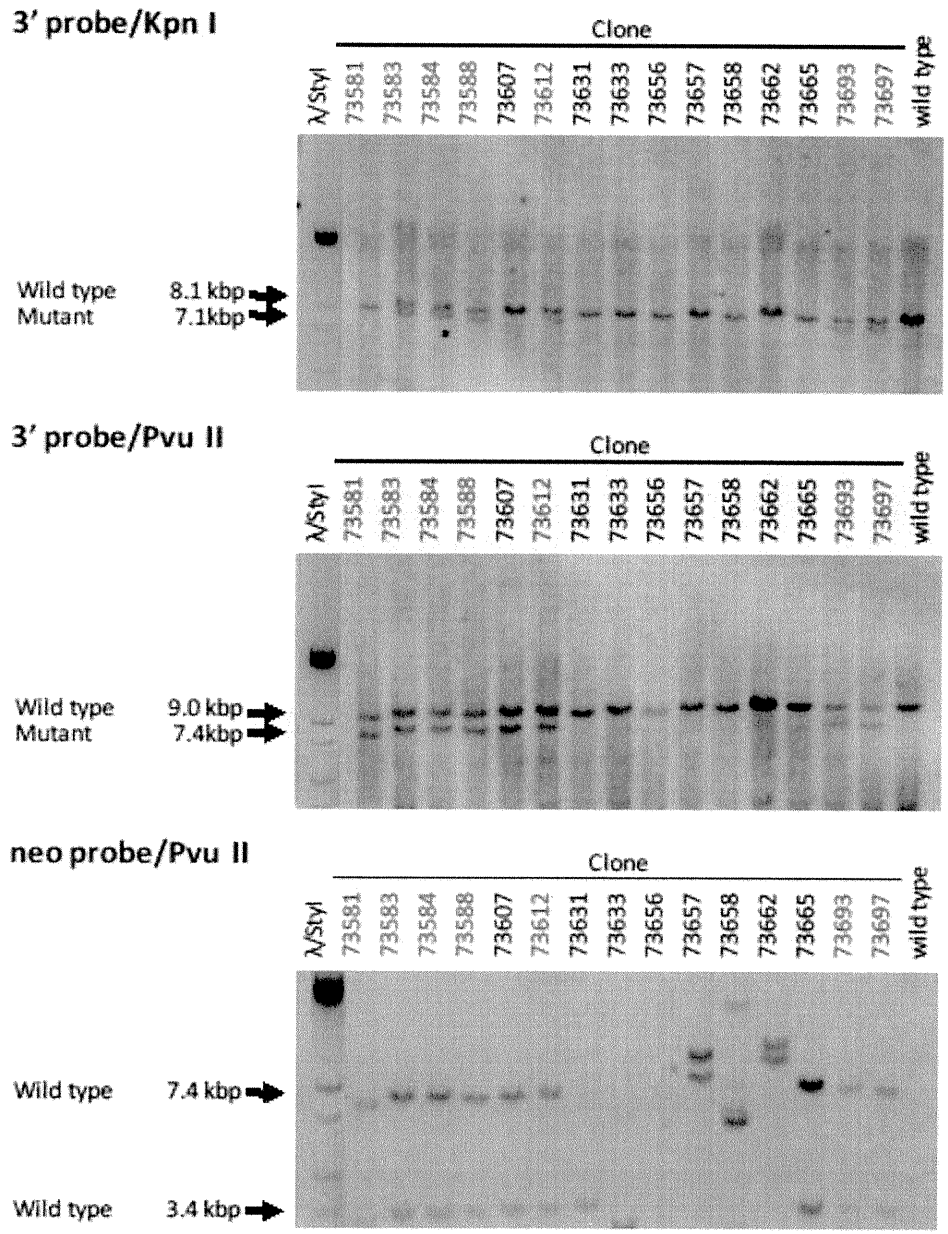

Figure S4 Kpn I/Pvu II-digested Southern blot analysis using 3'/neo probe

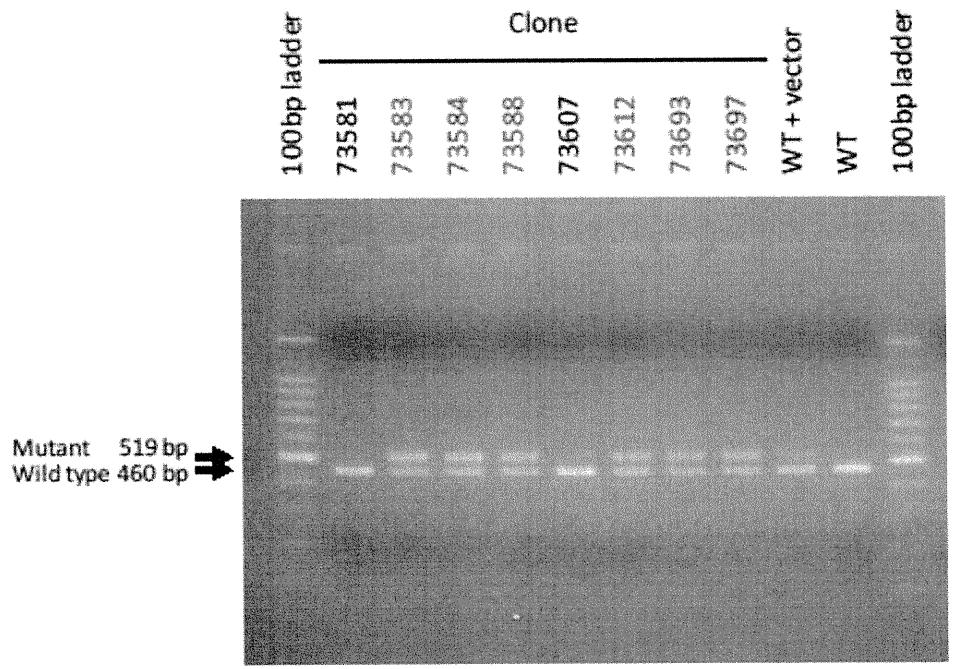

Figure S5 Agarose-gel electrophoresis of PCR products amplified with primer A and primer B

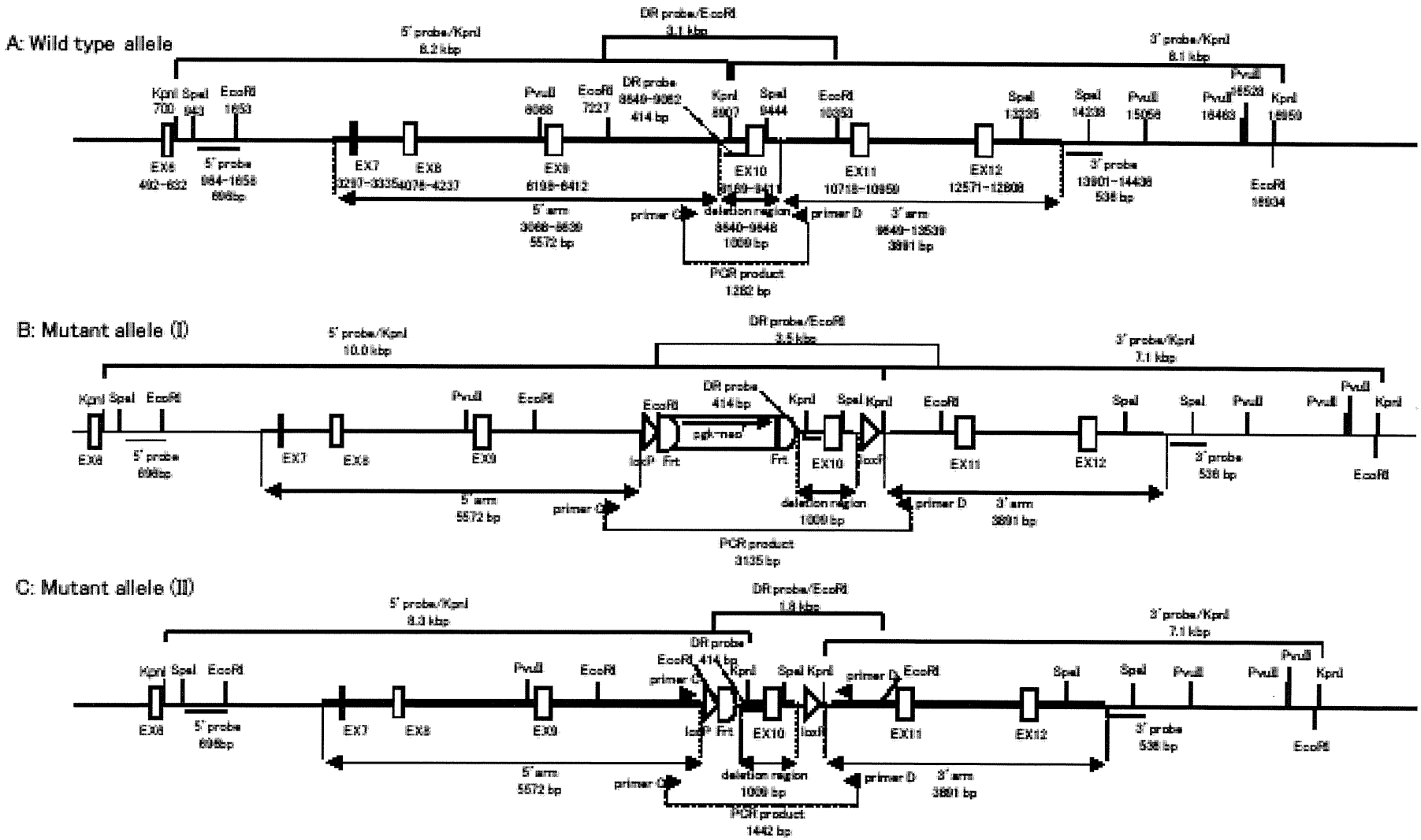

Figure S6 Eliminated the PGK-neo region by Flp recombination system

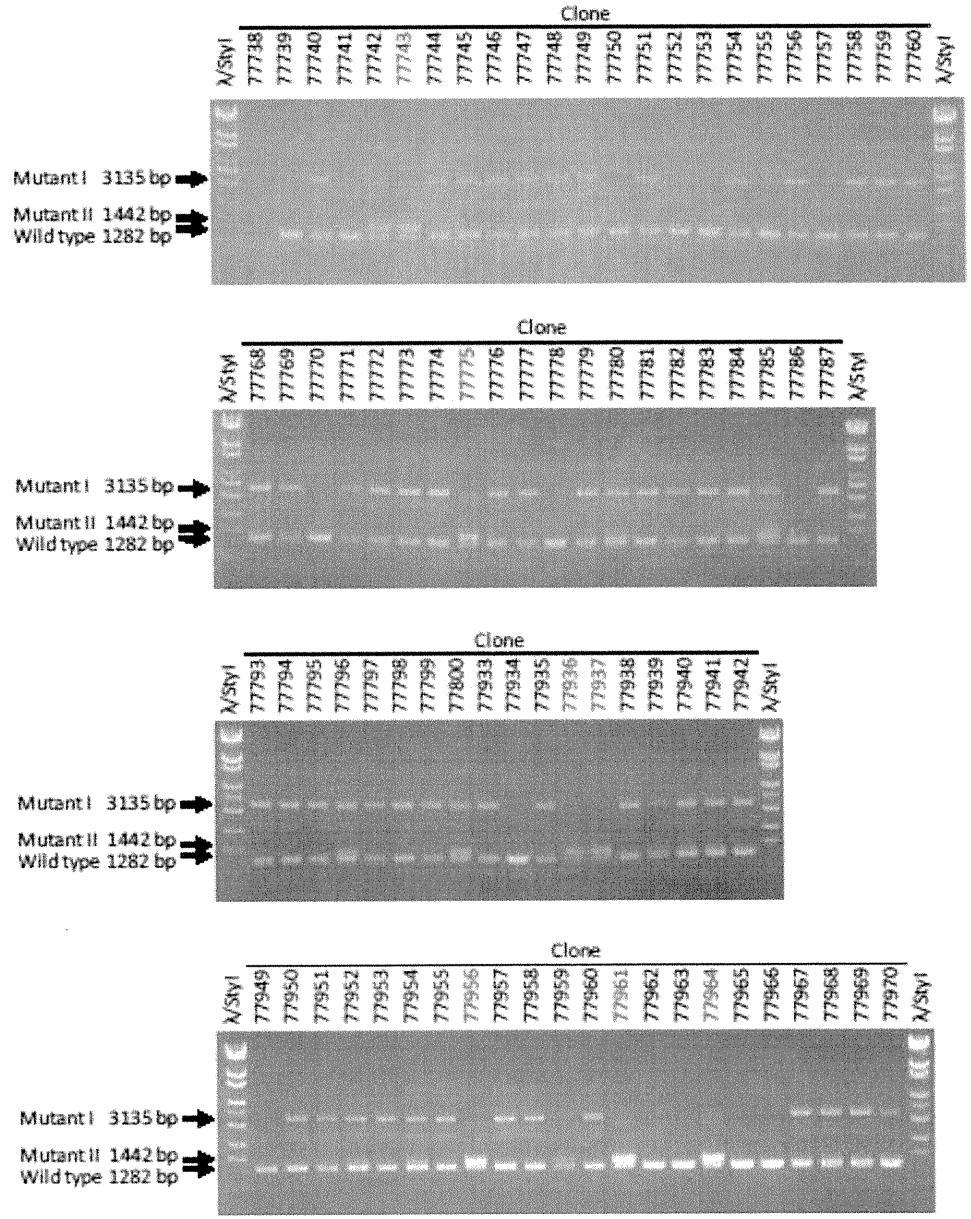

Figure S7 Agarose-gel electrophoresis of PCR products amplified with primer C and primer D

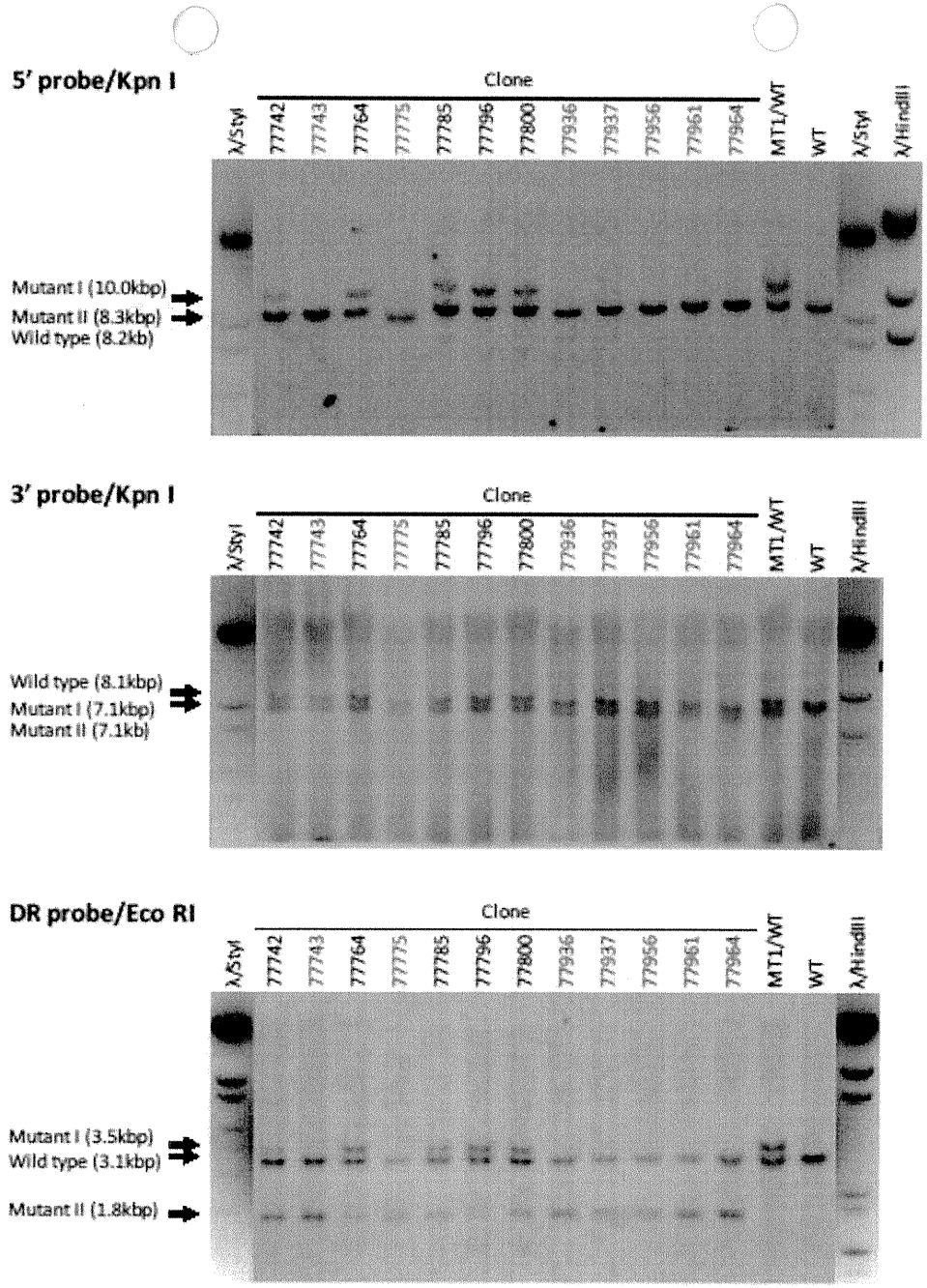

Figure S8 Kpn I/EcoRI-digested Southern blot analysis

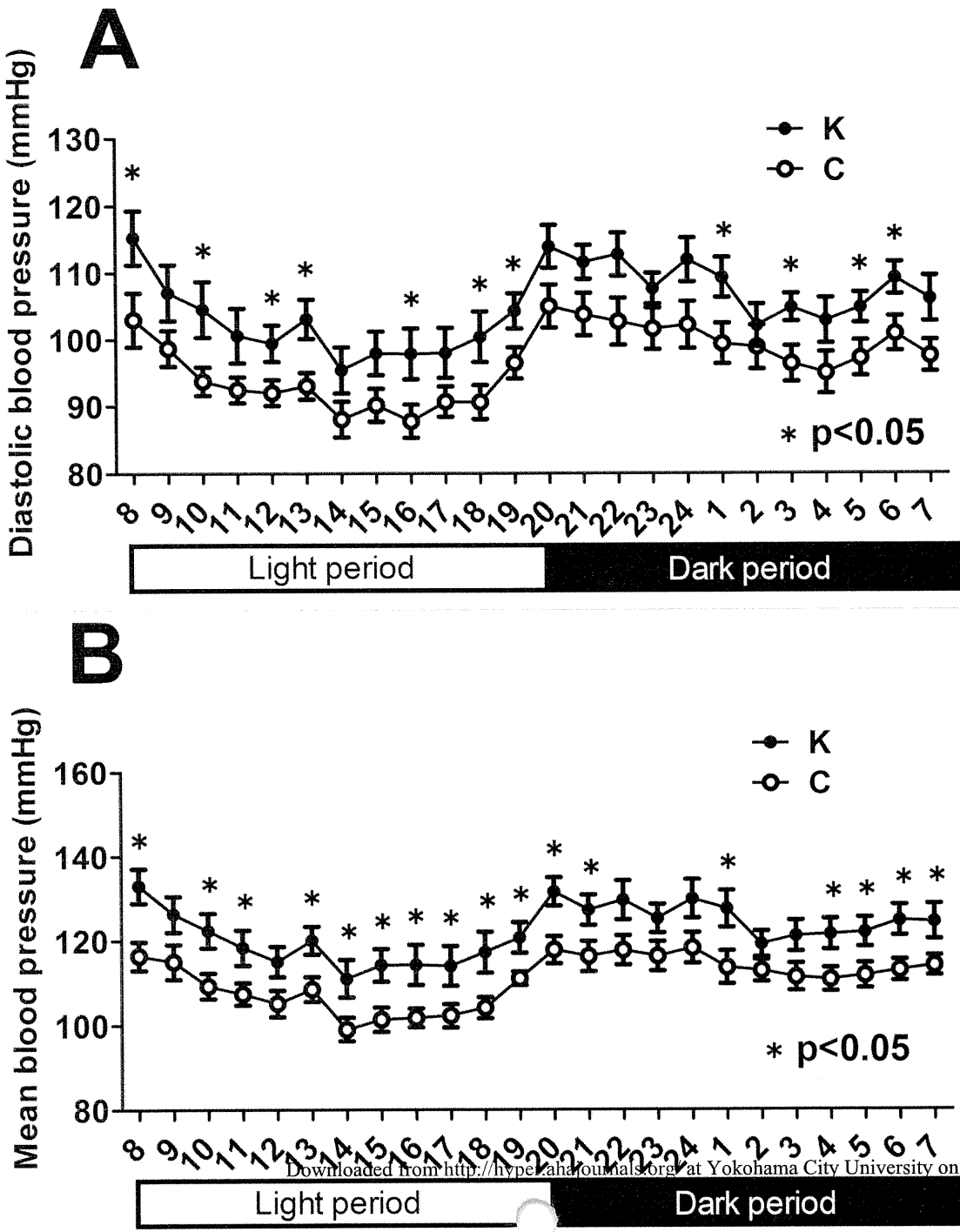

Figure S9 Diastolic and mean blood pressure measured by radiotelemetry

(A) Circadian patterns of diastolic blood pressure in VSMC ATP2B1 KO mice (n=9) and control mice (n=9) on a 12 hour light (8 AM to 8 PM) / dark (8 PM to 8 AM) cycle are shown. Mice were studied on a normal-salt diet. Values plotted are hourly means and standard errors measured over 60 hours (C: control mice, K: VSMC ATP2B1 KO mice). (B) Circadian patterns of mean blood pressure in VSMC ATP2B1 KO mice (n=9) and control mice (n=9) on a 12 hour light (8 AM to 8 PM) / dark (8 PM to 8 AM) cycle are shown. Mice were studied on a normal-salt diet. Values plotted are hourly means and standard errors measured over 60 hours.

THE JOURNAL OF BIOLOGICAL CHEMISTRY VOL. 286, NO. 22, pp. 19682–19692, June 3, 2011
Printed in the U.S.A.

Secretoglobin 3A2 Suppresses Bleomycin-induced Pulmonary Fibrosis by Transforming Growth Factor β Signaling Down-regulation*[S]

Received for publication, March 10, 2011, and in revised form, April 8, 2011 Published, JBC Papers in Press, April 10, 2011, DOI 10.1074/jbc.M111.239046

Reiko Kurotani[‡§¶], Satoshi Okumura[§], Tsutomu Matsubara[‡], Utako Yokoyama[§], John R. Buckley[‡], Takeshi Tomita[‡], Kyohei Kezuka[§], Tomokazu Nagano[‡], Dominic Esposito[‖], Troy E. Taylor[‖], William K. Gillette[‖], Yoshihiro Ishikawa[§], Hiroyuki Abe[¶], Jerrold M. Ward[‡‡], and Shioko Kimura[‡1]**

*From the [‡]Laboratory of Metabolism, NCI, National Institutes of Health, Bethesda, Maryland 20892, the [§]Cardiovascular Research Institute, Yokohama City University, Yokohama, Kanagawa, Japan 236-0004, [¶]Biochemical Engineering, Faculty of Engineering, Yamagata University, Yonezawa, Yamagata, Japan 992-8510, [‖]Protein Expression Laboratory, Advanced Technology Program, SAIC-Frederick, Inc. NCI, National Institutes of Health, Frederick, Maryland 21701, the **Cardiovascular Research Institute, Department of Cell Biology and Molecular Medicine and Medicine (Cardiology), New Jersey Medical School, University of Medicine and Dentistry of New Jersey, Newark, New Jersey 07103, and the [‡‡]Global VetPathology, Montgomery Village, Maryland 20866*

With increasing worldwide rates of morbidity and mortality of pulmonary fibrosis, the development of effective therapeutics for this disease is of great interest. Secretoglobin (SCGB) 3A2, a novel cytokine-like molecule predominantly expressed in pulmonary airways epithelium, exhibits anti-inflammatory and growth factor activities. In the current study SCGB3A2 was found to inhibit TGFβ-induced differentiation of fibroblasts to myofibroblasts, a hallmark of the fibrogenic process, using pulmonary fibroblasts isolated from adult mice. This induction was through increased phosphorylation of STAT1 and expression of SMAD7 and decreased phosphorylation of SMAD2 and SMAD3. To demonstrate the effect of SCGB3A2 on the TGFβ signaling *in vivo*, a bleomycin-induced pulmonary fibrosis mouse model was used. Mice were administered bleomycin intratracheally followed by intravenous injection of recombinant SCGB3A2. Histological examination in conjunction with inflammatory cell counts in bronchoalveolar lavage fluids demonstrated that SCGB3A2 suppressed bleomycin-induced pulmonary fibrosis. Microarray analysis was carried out using RNAs from lungs of bleomycin-treated mice with or without SCGB3A2 and normal mice treated with SCGB3A2. The results demonstrated that SCGB3A2 affects TGFβ signaling and reduces the expression of genes involved in fibrosis. This study suggests the potential utility of SCGB3A2 for targeting TGFβ signaling in the treatment of pulmonary fibrosis.

An increasing number of people are affected by pulmonary fibrosis worldwide, with increasing morbidity and mortality rates. In the United States, the number of patients suffering from pulmonary fibrosis is about 200,000 (1, 2) (www.nhlbi.nih.gov). Recovery from pulmonary fibrosis is possible at early stages of the disease, whereas the recovery is limited once the fibrosis has progressed. A risk for developing pulmonary fibrosis increases by administration of bleomycin (BLM),[2] an anticancer and antibiotic agent, used in therapy for many types of solid tumors.

Fibrosis arises from inflammation initiated by cell injury, and injured tissues are gradually replaced by collagen fibers that are produced from fibroblasts and accumulate as myofibroblasts. Damaged cells produce chemokines, which stimulate leukocytes to proliferate and produce profibrotic cytokines such as transforming growth factor β (TGFβ), a major profibrotic growth factor, and interleukin-13 (IL-13), a major profibrotic mediator. TGFβ1 induces collagen type I transcription through the SMAD signaling, whereas IL-13 stimulates macrophages to produce TGFβ (3–6). On the other hand, interferon-γ (IFNγ) inhibits collagen generation through STAT1 activation followed by sequestration of p300, which plays a pivotal role in the regulation of collagen synthesis by TGFβ (7, 8). IFNγ also induces the antagonistic SMAD7, which in turn impairs TGFβ signaling through inhibition of the SMAD3 interaction with the TGFβ receptor (9) and/or disruption of formation of the TGFβ-induced functional SMAD-DNA complex (10). Other molecules are also involved in the fibrotic process (6). These include other Th2 cytokines such as IL-4, IL-5, and IL-10, chemokines such as CCL2 and CCL3, connective tissue growth factor, and platelet-derived growth factor (3, 11). Molecules involved in various pathways leading to myofibroblast expansion are considered to be useful as therapeutic targets. To this end, a number of inhibitors and/or monoclonal antibodies against these targeted molecules have been developed and subjected to clinical trials as a means to treat fibrosis (3, 11, 12). IFNγ is one of the targeted molecules used as a new therapy for

* This work was supported by the National Institutes of Health, Center for Cancer Research (Intramural Research Program of the NCI; NIH 0010190305 and Z01 BC010449-06, to S. K.). This work was also supported by Grant-in-aid for Young Scientists (B) (21790207, to R. K.).

[S] The on-line version of this article (available at http://www.jbc.org) contains supplemental Table S1 and S2 and Figs. S1–S5.

All effective genes were submitted to the Gene Expression Omnibus (GEO: ID GSE21560, www.ncbi.nlm.nih.gov).

[1] To whom correspondence should be addressed: Bldg. 37, Rm. 3106, NIH, Bethesda, MD 20892. Tel.: 301-496-0958; Fax: 301-496-8419; E-mail: kimuras@mail.nih.gov.

[2] The abbreviations used are: BLM, bleomycin; SCGB, secretoglobin; CHX, cycloheximide; GO, gene ontology; MMPs, metalloproteinases; qRT, quantitative RT; BALF, bronchoalveolar lavage fluid; αSMA, α smooth muscle actin; rm, recombinant mouse.

fibrosis (5, 6, 12); however, because of potentially harmful side effects, a better alternative is desirable (13).

Secretoglobin (SCGB) 3A2, previously called uteroglobin-related protein 1, is a member of the SCGB gene superfamily (14). The SCGB gene superfamily consists of 3 gene families; family 1 has 4 subfamilies, each composed of 3–11 members, family 2 consists of 2 subfamilies, each with 6–10 members, and family 3 consists of only one subfamily with 5 members (15, 16). All members of the SCGB gene superfamily are cytokine-like secreted proteins of ~10 kDa, found only in mammals. They form homodimers or heterodimers with other members. Most functions of SCGB are still elusive, and the signaling pathways including a possible receptor(s) that transmits activities of these proteins is not known. Among the best studied member of the gene superfamily is SCGB1A1, also called uteroglobin, Clara cell secretory protein, or Clara cell 10-kDa protein that exhibits anti-inflammatory and immunomodulatory activities in lung (17–19). Studies on the mechanisms of the anti-inflammatory activity of SCGB1A1 have been carried out (20, 21). Other members such as SCGB2A2 (mammaglobin A) and SCGB1D2 (lipophilin B) are known as a cancer marker for mammary gland (22) (23).

SCGB3A2 is the second member of the SCGB family 3, subfamily A. It is predominantly expressed in lung airways. SCGB3A2 was found to play a role in suppression of lung inflammation using a mouse model for allergic airway inflammation (24) and to promote branching and maturation of mouse fetal lungs (25). MARCO (macrophage scavenger receptor with collagenous structure), expressed in alveolar macrophages in lung, was suggested as a possible receptor for SCGB3A2 (26). On the other hand, we have demonstrated the possible presence of a SCGB3A2-specific receptor on the mesenchymal cells of mouse fetal lungs (25). Despite these studies, very little is known about the biological and physiological functions of SCGB3A2 and its mechanisms of action including the receptor and the signaling pathway it provokes.

In the present study SCGB3A2 was found to inhibit the TGFβ signaling through increased STAT1 phosphorylation and expression of SMAD7 and decreased phosphorylation of SMAD2/3, thus resulting in inhibition of TGFβ-induced myofibroblast differentiation. In an *in vivo* mouse model, SCGB3A2 markedly suppressed BLM-induced pulmonary fibrosis, suggesting the potential use of SCGB3A2 as a novel therapeutic reagent to treat pulmonary fibrosis.

EXPERIMENTAL PROCEDURES

Isolation and Primary Culture of Lung Fibroblasts—Lung tissues from 7–9-week-old female mice were cut into small pieces, mounted on collagen type I-coated 60-mm plate (IWAKI, Shizuoka, Japan), and then cultured for 7 days. Fibroblasts were harvested by 0.5% trypsin and 0.53 mM EDTA in PBS, washed with DMEM supplemented with 10% FBS, plated on a 35-mm plate, and cultured for 16 h. Fibroblasts were stimulated by 10 ng/ml TGFβ (Sigma) in DMEM containing 3% FBS for 24–72 h in the presence or absence of recombinant mouse (rm) SCGB3A2 (2.5 μg/ml). The recombinant mouse SCGB3A2 (rmSCGB3A2) was purified as described (25) (detailed purification method of SCGB3A2 will be provided upon request). For simplicity "SCGB3A2" is used instead of rmSCGB3A2 throughout the manuscript. For blocking experiments of IFNγ receptor signaling, a specific antibody against IFNγ receptor (rat anti-CD119 clone GR20, BD, Tokyo, Japan) was co-cultured with SCGB3A2 or IFNγ (R & D Systems, Minneapolis, MN) for 24 h or 30 min, respectively. To determine translational regulatory mechanism, fibroblasts were incubated with SCGB3A2 (2.5 μg/ml) and cycloheximide (CHX, 1 μg/ml, WAKO, Osaka, Japan) for 3 h or pretreated with CHX 3 h before stimulation with IFNγ. To down-regulate Stat1 expression, Stat1 siRNA probes (no. 7 probe, sense strand (5′-GCAUCUUACUGAAGGUGAATT-3′) and antisense strand (5′-UUCACCUUCAGUAAGAUGCAT-3′) and no. 8 probe (sense strand 5′-GAGUUGGUUUAAUAUAUAUTT-3′) and antisense strand (5′-AUAUAUAUUAAACCAACUCAT-3′); Qiagen, Valencia, CA) were transfected into fibroblasts using Lipofectamine 2000 (Invitrogen) 48 h before addition of TGFβ and/or SCGB3A2.

Immunoblotting—Immunoblotting was performed using the following antibodies; anti-STAT1, anti-pSTAT1 (Tyr-701), anti-SMAD2, anti-pSMAD2 (Ser-465/467), anti-SMAD3 (Cell Signaling Technology, Danvers, MA), anti-pSMAD3 (Ser-423/425) (Millipore Corp. Temecula, CA), anti-SMAD7 (Santa Cruz Biotechnology, Inc. Santa Cruz, CA), anti-α-smooth muscle actin (αSMA; Sigma), and anti-β-actin (Sigma). Immunoblotting was performed as described in Kurotani *et al.* (25). All immunoreactive bands were visualized using ECL (GE Healthcare) or ImmunoStar LD (WAKO) with LAS-3000mini (FUJIFILM, Tokyo, Japan) and then standardized by immunoreactive band of β-actin using Multi Gauge Version 3.0 software (FUJIFILM).

Quantitative RT-PCR and RT-PCR—Total RNAs isolated using TRIzol (Invitrogen) and digested with DNase I were reverse-transcribed by Superscript II reverse transcriptase (Invitrogen). Quantitative RT-PCR (qRT-PCR) was performed with ABI Prism 7900 Sequence Detection System (Applied Biosystems, Foster City, CA) using SYBR Green master mixture. The standard curve method was used, and all data were normalized to 18 S rRNA amplified using TaqMan Ribosomal RNA Control Reagent, VIC Probe (Applied Biosystems). RT-PCR was performed using AmpliTaq Gold DNA polymerase (Applied Biosystems) with iCycler (Bio-Rad). PCR condition used was 50 °C for 2 min and 95 °C for 10 min followed by 95 °C for 15 s and 60 °C for 40 s for 40 cycles. Primers used for qRT-PCR and RT-PCR analysis are summarized in supplemental Table S1. Leukocytes isolated from normal mouse spleen were stimulated by phorbol 12-myristate 13-acetate, (10 ng/ml) (Calbiochem) and ionomycin (1 μM) (Calbiochem) for 3 h or by poly(I:C) (polyinosinic-polycytidylic acid potassium salt, 10 μg/ml; Imgenex, San Diego, CA) for 24 h. The mRNAs extracted were used as a positive control for IFNγ and IFNα (27) and for IFNβ, respectively (28).

Animals and SCGB3A2 Treatment—C57BL/6N mice (NCI-Frederick, National Institutes of Health) were maintained under a standard 12-h light/12-h dark cycle with water and chow provided *ad libitum*. At least ten 7–8-week-old C57BL/6N mice were prepared for each group. Eight units/kg BLM (Sigma) or PBS was directly administered once by intratracheal intubation into C57BL/6N mice using the BioLITE sys-

tem (BioTex, Inc., Houston, TX). Purified SCGB3A2 (1.5 mg/kg/day) or PBS was intravenously administered to mice via the tail vein once daily for a week starting on day 14 after BLM administration. Four groups of mice were used in this study; administration of BLM followed by intravenous injection of PBS (Group 1) or SCGB3A2 (Group 2) or administration of PBS followed by intravenous injection of PBS (Group 3) or SCGB3A2 (Group 4). All animal studies were performed after approval by the National Cancer Institute Animal Care and Use Committee. SCGB3A2 used in the animal study contained endotoxin at 0.2 enzyme units/mg. The dose of SCGB3A2 was determined based on the previous study in which a total of 200 μg, but not 100 μg, exhibited growth factor activity without causing any gross abnormalities to the dam as well as the embryos (25). For microarray analysis, C57BL/6N mice (7–8 weeks old) were treated with PBS or SCGB3A2 by intravenous administration and were euthanized 12 h later.

Bronchoalveolar Lavage—On day 21 after administration of BLM, mice were euthanized and subjected to bronchoalveolar lavage. Bronchoalveolar lavage fluid (BALF) was obtained by intratracheal instillation of 1 ml of PBS into the lung while it was kept in the thoracic cavity. Cells in the BALF were centrifuged at 500 × *g* and subjected to Diff-Quick (Baxter Healthcare, Miami, FL) staining. Cells were identified and counted using 2000–2500 cells from 10 fields randomly chosen. Tissues were fixed in 4% paraformaldehyde or stored at −80 °C for later RNA preparation.

Pathology—The whole lung was inflated and fixed with 4% paraformaldehyde. Lung tissues were embedded in paraffin, and 4-μm whole lung sections were prepared. Hematoxylin and eosin staining was carried out for assessment of BLM-induced fibrosis. Masson's Trichrome staining (Sigma) was used to detect collagen fibers. Immunohistochemical staining for SCGB3A2, pSMAD2, pSMAD3, and SMAD2/3 was performed in BLM-treated lungs using anti-mouse SCGB3A2 antibody (produced in our laboratory) (14), anti-pSMAD2(ser465/467) (Cell Signaling Technology), anti-pSMAD3 (Epitomics, Burlingame, CA), and anti-SMAD2/3 (BD Biosciences), respectively. For antigen-retrieval, the sections were incubated in Tris-EDTA (pH 6.0) at a temperature over 95 °C for 10 min before protein blocking. The immunoreactivities were enhanced by ABC method (Vector Laboratories, Burlingame, CA) followed by visualization using diaminobenzidine (DakoCytomation, Carpinteria, CA) and counterstained with hematoxylin. Immunocytochemical staining for αSMA was performed as described (29, 30). Briefly, fibroblasts cultured on 8-well Lab Tek Chamber Glass Slide (Nalge Nunc International, Naperville, IL) with and without TGFβ and/or SCGB3A2 were incubated at room temperature in PBS containing 0.1% Triton X 100 for 15 min followed by fixing with 4% paraformaldehyde for 15 min at room temperature. Cells were incubated with anti-αSMA antibody (Sigma, 1:400) overnight at 4 °C after blocking with 3% BSA-PBS for 1 h at room temperature. Cells were incubated with Alexa Fluor 488 goat anti-mouse IgG (Invitrogen) for 30 min at room temperature in dark. Nuclei were stained by 1 mg/ml DAPI (4′,6-diamino-2-phenylindole) (47). The αSMA signal was observed using Nikon EC (Nikon, Tokyo, Japan).

Fibrosis Assessment (Grading)—The grade of BLM-induced pulmonary fibrosis was determined based on the percentage of the fibrotic area in the whole lung section as follows; the presence of fibrosis in 0–25% of the lung for Grade 1, 26–50% of the lung for Grade 2, 51–75% of the lung for Grade 3, and 76–100% of the lung for Grade 4. No fibrosis, but with inflammation including a few infiltrating foci of lymphocytes or a very small granulomas, was considered Grade 0.

DNA Microarray—Total RNAs were purified using TRIzol and RNAeasy (Qiagen, Valencia, CA) from lungs of four groups (Group 1, 2, 3, and 4) of mice as described above or mice 12 h after SCGB3A2 treatment. Ten (group mice analysis) or 20 μg (SCGB3A2 treatment) of purified total RNA were reverse-transcribed to label with Cy3 and Cy5 (GE Healthcare) using the FairPlay Microarray Labeling kit (Stratagene, La Jolla, CA) or SuperScript™ Indirect cDNA Labeling Core kit (Invitrogen), respectively. Microarray analysis was carried out using individually isolated RNA from at least 5 mice in each group and mouse array chips (45K) obtained from the NCI Microarray Facility. Experiments and analysis were performed according to the manufacturer's instruction and the instruction of the Center for Cancer Research, NCI (nciarray.nci.nih.gov). Gene Ontology (GO) analysis (31) and pathway analysis were performed using a mouse gene data (Mm-Std_20060628.gdb) and a mouse pathway data (Mm_Contributed_20070917) from MAPPFinder (32). Up-regulated genes were sorted based on scores (ratio of Cy5 per Cy3) more than 2.0 (average) between Group 1 and Group 3, more than 1.5 (average) between Group1 and Group2, and those up-regulated in all reactions.

Statistical Analysis—Data are shown as the mean ± S.D. from indicated numbers of independent experiments. Statistical analysis was performed one-way ANOVA followed by Bonferroni multiple comparison test.

RESULTS

Effect of SCGB3A2 on Differentiation of Fibroblasts into Myofibroblasts—It was previously demonstrated that SCGB3A2 has at least two biological functions; an anti-inflammatory function was revealed using an ovalbumin-induced allergic airway inflammation model (24), and growth factor activity was studied using *ex vivo* fetal lung organ cultures and *in vivo* injection of SCGB3A2 to pregnant mice (25). To obtain insight into whether SCGB3A2 plays any additional roles in lung physiology and/or diseases, primary fibroblasts obtained from adult mouse lungs were used as an *in vitro* model of fibrosis in which the effect of SCGB3A2 on TGFβ-induced differentiation of fibroblasts into myofibroblasts was studied (33). Inhibition of this transformation would indicate a role for SCGB3A2 in controlling fibrosis. As expected, TGFβ treatment resulted in differentiation of pulmonary fibroblasts to myofibroblasts within 24 h as clearly seen by the characteristic myofibroblast morphology and the robust expression of αSMA (Fig. 1*A*, *TGFβ*, αSMA is seen in *green*). In contrast, treatment of fibroblasts with both TGFβ and SCGB3A2 together (TGFβ+SCGB3A2) exhibited morphology and the level of αSMA expression similar to those of normal fibroblasts (Fig. 1*A*, *Cont. versus TGFβ+SCGB3A2*). SCGB3A2 alone did not have any effect on the morphology of fibroblasts (Fig. 1*A*, *SCGB3A2*). Note that the number of cells